A Model-based Parametric Study for Comparison of System Configurations and Control of a Hydrogen Hybrid Cargo Vessel

Foivos Mylonopoulos[a*], Timon Kopka[a], Andrea Coraddu[a], and Henk Polinder[a]

[a] Department of Maritime and Transport Technology, Delft University of Technology, 2628 CD Delft, The Netherlands
* Corresponding Author: F.P.Mylonopoulos@tudelft.nl

Abstract
The current state of research in marine energy systems has concentrated on conventional diesel systems, while limited literature is available on the configuration and control of alternative energy sources such as hydrogen hybrid systems, which have attracted increasing interest recently owing to the energy transition. This paper presents a modelling and control study for conceptual retrofitting of a general cargo vessel to a hydrogen-hybrid version. Generic fuel cell, battery, and converter models are used, enabling easy adaptation to various powerplant sizes and ship types. A robustly coordinated Energy Management Strategy (EMS), which can be implemented for different vessel's power profiles, was developed for power sharing, DC bus voltage control, and battery State of Charge (SoC) regulation. The total installed fuel cell power and battery capacity were heuristically selected from a range of power profiles of the ship. A database of fuel cells with stacks from different manufacturers was created to test different combinations in terms of fuel consumption, cost, and weight, based on the framework of the problem. Uncertainties in terms of fuel prices are presented using normal distribution graphs. The system configurations and control results are presented for one power profile of the vessel and the average fuel costs. It is demonstrated that with the proposed control method, the power losses are less than 1%, the DC bus voltage fluctuations are less than 0.5%, and the battery SoC remains between 35-65% for the entire duration of the analysed power profile. The configuration with eight stacks of 150 kW has the lowest total fuel cost (730 $) with an average difference of 7.1% from the other solutions, and the lowest total weight (10.54 tons) with an average difference of 15.4% from the other configurations. Overall, this study demonstrates the efficient configuration and control of hybrid energy systems using parameterized components.

Keywords: Cargo Ship**,** Configurations**,** Control, Cost Uncertainties, Hydrogen--Fuel Cells, Parametric Study.

1. INTRODUCTION

The shipping industry is responsible for 3% of global Greenhouse Gas emissions. However, if no countermeasures are taken, this percentage may increase to 17% by 2050 [1]. Thus, the International Maritime Organization has imposed stringent regulations requiring a 50% emission reduction by 2050 compared to the 2008 levels [1]. One of the most promising alternative fuels for emission reduction is hydrogen, which can result in zero onboard emissions if fuel cells are utilised. They are scalable power sources with high efficiency at their rated level, and they produce power with reduced noise and vibrations compared to conventional engines without emitting harmful gases. Hybrid configurations of fuel cells and batteries have attracted increasing interest in recent years [2]. Batteries are used to cover the peak demands and transient loads that fuel cells cannot deliver owing to their limited power output and slow response. Such hydrogen hybrid configurations are more applicable for short ranges near recharging and refuelling infrastructure. Despite their higher cost and complexity compared to traditional configurations with diesel mechanical propulsion, hydrogen-hybrid systems offer increased flexibility, energy efficiency, and reliability in the case of failures [3].

Currently, most studies have focused on the modelling, control, and optimization of diesel-based (hybrid) ship systems because they have been in use for a long time and are well-established in the marine sector. In most cases, the objective is to increase the use of renewable sources by reducing the operation of diesel generators/engines to minimize onboard emissions. Zhu *et al*. [4],[5] modelled and optimized the sizes of the batteries,

@2023 Mylonopoulos, F. et al., published by TU Delft OPEN Publishing on behalf of the authors. Licensed under a Creative Commons Attribution CC BY license.
DOI: https://doi.org/10.59490/ moses.2023.671

generators, and e-motors of a diesel electric vessel using the Non-dominated Sorting Genetic Algorithm to reduce emissions, lifecycle costs and diesel consumption.

Vu *et al*. [6] proposed a Power Management Strategy using the interior point algorithm to optimally control the load splitting between the diesel generators and batteries of a hybrid tugboat.

Kanellos *et al*. [7],[8] developed models and control strategies using Particle Swarm Optimization algorithms to reduce the operational expenses and satisfy the emission requirements (operational indexes) for the case vessels.

The authors of [9],[10] modelled and sized the diesel generators, batteries, and supercapacitors to optimally control the highly fluctuating loads of the power profiles of vessels.

The modelling, control, and optimization studies for hydrogen-based vessels have focused on passenger vessels (i.e., small boats, high-speed ferries, roll-on-roll-off vessels). Because there are no emissions onboard, more focus is given to operational costs, capital expenses, and degradation of components.

Different studies have used the generic fuel cell and battery models from the Simscape library, which are also used in this study, focusing mainly on system control. Balestra and Schjølberg [11],[12] modelled the powertrain of a conceptually retrofitted hydrogen-based passenger vessel using real ship data. They tested the effects of component sizes on different Energy Management approaches, with a focus on hydrogen cost and component degradation.

Jaster *et al*. [13] modelled the propulsion and control systems of a hydrogen vessel and simulated them using the hardware-in-the-loop method to estimate the loads and fuel consumption.

Cha *et al*. [14] used an optimisation-based approach for the power management to maximize the efficiency of the fuel cells while constraining the battery State of Charge (SoC).

Bassam *et al*. [15] presented a multi-scheme Energy Management Strategy (EMS) that could switch to different control approaches based on the pre-defined instructions for varying battery SoC and operating profile, aiming to minimize the energy consumption.

Bassam *et al*. [16] presented an improved Proportional Integral strategy for a hydrogen-hybrid tourist boat and compared the optimization results of hydrogen consumption, cost, and component stresses with three other approaches: Classical Proportional Integral, Equivalent Consumption Minimization Strategy, and a rule-based method.

A summary of the main points and learnings from the above-mentioned studies, and the literature gaps addressed in this research are presented herein. There have been many studies on the design and control of diesel-based ship systems but very few have focused on system configurations and control for hydrogen hybrid vessels. In most cases, one fuel cell stack is considered for the analysis, with specifications from a specific manufacturer, without comparing the different system arrangements and fuel cell models in terms of fuel consumption and weights. To the best of the authors' knowledge, there are no studies on the selection of component sizes, configurations, and system control for vessels with multiple operating conditions and power profiles. Studies on hydrogen-hybrid ships usually consider a passenger vessel with a fixed route, schedule, and one power profile for the analysis, which simplifies the selection of component sizes and the EMS approach. Simple rule-based or PI-based approaches are usually implemented with a focus on power sharing between the components to minimize the energy losses for the considered load profile.

This is a model-based parametric study using generic fuel cell/battery models and average converters. A diesel-based general cargo vessel was conceptually retrofitted to a hydrogen-based version with hybrid power supply. Low-temperature proton-exchange membrane fuel cells and lithium-ion batteries are the power supply sources and electric motors are used for propulsion. The aim of this research is to compare different configurations of fuel cells and batteries in terms of fuel consumption/cost and weight, and to efficiently control the systems. The novelties and contributions of this study are summarized as follows. To the best of the authors' knowledge, this is the first such analysis for a general cargo vessel with various power profiles. A robustly coordinated EMS, that can be applied to different vessel profiles, was developed to control the DC bus voltage, SoC and for efficient power sharing. The installed fuel cell power and battery energy capacity were heuristically selected from a range of power profiles derived from real-time onboard measurements. Different combinations of fuel cells and batteries from various manufacturers were tested in terms of fuel consumption/cost, weight, Uncertainties in the fuel prices were considered for the calculations. The system configurations and control results are presented for one power profile of the vessel and the average hydrogen costs.

The remainder of this paper is organised as follows. In Section 2, the case study details for the vessel and its operating profiles are presented. The

proposed methodology, models and controllers are described in Section 3. The results of the simulations and discussions are presented in Section 4. Finally, the concluding remarks and directions for future research are presented in Section 5.

2. CASE STUDY

The specifications of the general cargo vessel considered in the analysis are listed in Table 1. The original version had one main diesel engine and a controllable pitch propeller.

Table 1. Case vessel specifications

Parameters	Values/Info
Length	89.9 m.
Width	12.5 m.
DWT	3638 t.
Year built	2007
Engine	Wartsila 9L20

The general cargo vessel does not have a fixed schedule and route. Instead, there are different operational areas and power profiles. The most energy-intensive (load fluctuating) and power-intensive load profiles are shown in Figure 1.

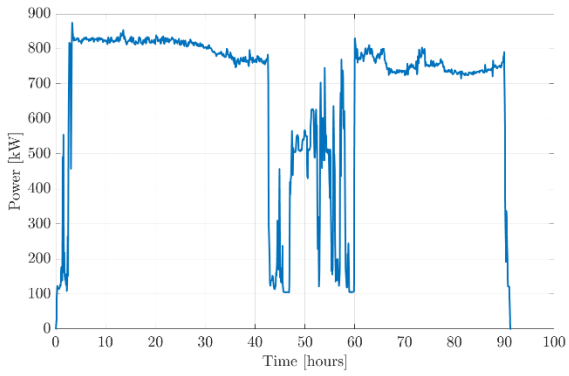

a) Energy intensive profile

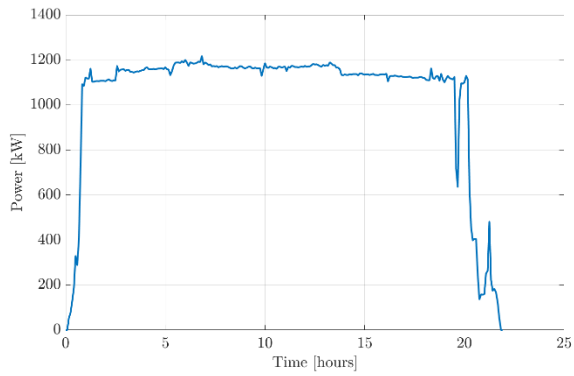

b) Power intensive profile

Figure 1: Power demand over time of the case vessel for different operating profiles

Data measurements were obtained for the propulsion loads from the main diesel engine of the original mechanical version of the cargo vessel with a frequency interval of 5 minutes. The engine's power output is the propulsion power demand for the retrofitted hydrogen-hybrid version developed in this study. The auxiliary loads have not been considered for the analysis since no measurement data is available.

3. METHODOLOGY

3.1 Framework

A simplified diagram of the methodology used in this study is shown in Figure 2. Detailed discussions of how the proposed methodology is applied to this case study are also presented in this section.

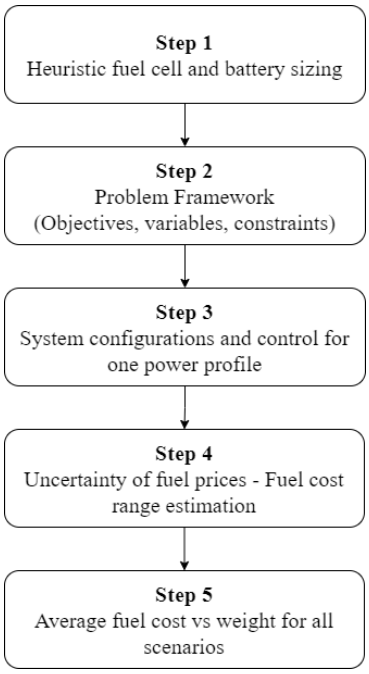

Figure 2: Steps of the proposed methodology

In the hydrogen version, the fuel cells and the batteries were sized according to the numerous power profiles of the vessel (Step 1). The sizes of the fuel cells, which are the main power sources, are such that they can cover the maximum recorded power output of 1200 kW (Figure 1b). The batteries were sized to deliver the highly fluctuating loads for energy-intensive profiles (Figure 1a). The selection of pack sizes was based on discussions with the vessel operators and industry experts. It was suggested that battery packs with a total energy capacity of 550 kWh and a total power of 800 kW could be sufficient for the

case vessel, considering its various operating profiles.

In Step 2, the problem framework is defined in terms of variables (i.e., number of batteries, number of fuel cells, and module selections from different manufacturers), objectives (i.e., fuel consumption/cost and system weight), and constraints. In particular, the following constraints were considered:

- $\text{Bus Voltage} = 1000\,\text{V} \pm 5\%$ [11]
- $20\% \leq \text{SoC}\,(t) \leq 80\%$ [12]
- $P_L(t) \leq P_{out}(t) \leq 1.01 P_L(t)$

where $P_L(t)$ is the power demand (load) as a function of time, and $P_{out}(t)$ is the combined power output of the fuel cells and batteries as a function of time. The upper limit of the power output was constrained to be up to 1% higher than the load demand to minimize the power losses.

In Step 3, different combinations of batteries and fuel cells were tested to estimate the fuel consumption, costs, weights, and to control the voltage and power levels. The analysis was performed for one profile of the vessel, which is presented in Section 4.1.

In Step 4, variable and uncertain fuel prices are considered. The fuel cost range was obtained by multiplying the fuel price by the fuel consumption for each scenario. The mean and standard deviation for each case with a 95% confidence interval were also considered.

Finally, in Step 5, the average fuel costs were plotted against the system weights for all the considered scenarios. The results of the fuel consumption and system weights were compared with those of the original diesel-based version.

The different scenarios for the modelling, design, and control analysis of the considered power profile are discussed in Section 4.1.

3.2 Models and control approach

A simplified diagram of the powertrain layout for 'n' components is shown in Figure 3.

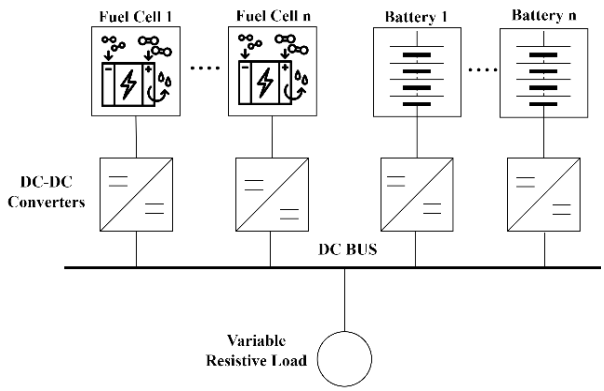

Figure 3: Powertrain configuration with varying number of fuel cells, converters, and batteries

Generic fuel cell and battery models from [17] and [18] respectively, have been used for modelling and integration of the systems into one powertrain. Average converter models have also been implemented, instead of detailed converters with pulse width modulation that would significantly increase the computational time. For system-level modelling, average models are sufficiently accurate [16].

The fuel cells are connected to the DC bus via unidirectional DC-DC converters, which increase the variable fuel cell voltage to the levels of the DC bus (1000 V).

For the batteries, the bi-directional converters enable discharging or charging onboard depending on the load demand. In this study, shore-charging was not considered. The DC bus is modelled with a single capacitance, which is obtained by the summation of all capacitances from the parallel-connected converters. The DC bus is connected to a single variable resistive load, which is equal to the bus voltage divided by the load current from the power profile.

The components after the DC bus, including inverters, AC motors, and propellers were not modelled in this study.

The implemented EMS developed for system control is shown in Figure 4.

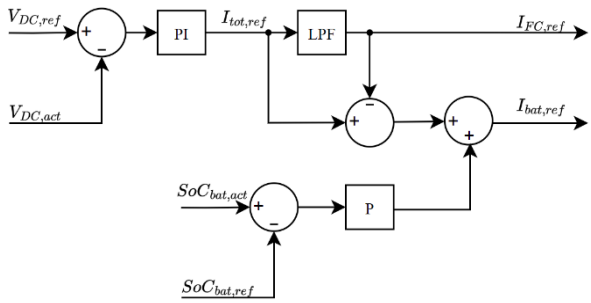

Figure 4: Developed EMS for power sharing, DC bus voltage control, and battery SoC regulation

In Figure 4, the DC bus voltage is controlled by a PI controller to its reference value of 1000 V. The total current output from the voltage regulation is then split into a low-frequency component for the fuel cells and a high-frequency component for the batteries. A low-pass filter is used before the fuel cell to limit the current gradients for degradation purposes [19]. The higher the time constant in the transfer function of the low-pass filter, the slower the fuel cell response and the smaller the fuel cell degradation. However, for a high time constant, the

batteries provide more power and degrade faster. A saturation block ensures that the fuel cell current remains within its limits. The fuel cell reference current is then split equally to the unidirectional DC-DC converters for current control.

The difference between the total current and fuel cell current is the battery current. For the batteries, the SoC is controlled with a P controller around a reference value of 50%, which is in the middle of the desired operating range of 20-80%. The P controller resulted in reduced oscillations compared to a PI controller around the equilibrium point. A PI controller with a high integral gain could be used if the aim was to keep the SoC almost constant at 50% SoC, but this would result in higher fuel consumption and fuel cell degradation, because almost all the power would be provided by the fuel cell stacks. With the P controller, if the SoC is below 50%, the system requires additional current to increase the SoC. The total battery current is a superposition of the voltage regulation and SoC regulation parts, and it is then split equally to the bi-directional converters of the battery packs that are connected in parallel. The SoC controller has much slower dynamic capabilities than those of the DC bus voltage controller. The limits for the battery charge and discharge currents are set in a saturation block. The developed EMS is robust and can be used for different power profiles of the vessel, because if the load profile changes, the fuel cell and the battery react to these changes.

The gains k_p and k_i for the DC bus voltage PI controller were estimated based on (1) and (2) as demonstrated in [20].

$$k_{p,DC} = \mathrm{C_{DC}}/\tau_{DC} \tag{1}$$

$$k_{i,DC} = 0.25k_{p,DC}^2/(4\mathrm{C_{DC}}) \tag{2}$$

where $k_{p,DC}$ and $k_{i,DC}$ are the proportional and integral gains, respectively, $\mathrm{C_{DC}}$ is the capacitance of the DC bus and τ_{DC} is a time constant for the voltage control which is set to 0.01 seconds for this study based on the authors' experience.

The gain of the P controller for battery SoC control was estimated based on (3) and (4).

$$k_{p,SoC} = \mathrm{I_{max}}/\Delta_{SoC} \tag{3}$$

$$\mathrm{I_{max}} = P_{Batt,max}/V_{DC} \tag{4}$$

where $k_{p,SoC}$ is the proportional gain of the SoC controller, $\mathrm{I_{max}}$ is the maximum battery current, Δ_{SoC} is the difference between the actual and reference SoC values, $P_{Batt,max}$ is the maximum battery power, and $\mathrm{V_{DC}}$ is the reference DC bus voltage which is 1000 V in this study.

3.3 Database of components

To test the different component sizes and system configurations, a small database of five actual fuel cell components with various power levels from different manufacturers was developed, as shown in Table 2.

Table 2. Fuel cell database

Components	Rated power (kW)	Stack weight (kg)
Zepp.Y50 [21]	50	212
HyPM HD90 [22]	100	327
Zepp. X-150 [21]	150	355
Powercell-200 [23]	200	1070
HyPM HD180 [22]	200	654

For the batteries, a single lithium-ion module from Toshiba was considered for the analysis [24]. The specifications of the modules are listed in Table 3.

Table 3. Battery module specifications

Parameters	Values (units)
Nominal voltage	24.6 V.
Rated capacity	45 Ah.
Weight	14.6 kg.

These modules are composed of numerous cells, and can be connected in series to increase the nominal voltage of the battery pack and in parallel to increase its rated capacity. The total installed energy capacity of the batteries was set equal to 550 kWh, as discussed in Section 3.1. Different numbers of battery packs were considered, ranging from 2 to 5 units, to investigate which configuration provides the required capacity with the lowest weight. A configuration with one battery pack was not considered because of the active redundancy requirements. Different total battery energy capacities will be considered in future work, where the optimal number and power/energy of components will be evaluated using an optimization algorithm.

4. RESULTS AND DISCUSSION

In this section, the results from the simulations are presented and discussed.

4.1 System configurations and control using the developed Energy Management

The analysis was conducted for a short power profile of 4.16 hours (15000 seconds) for computational reasons (Figure 5).

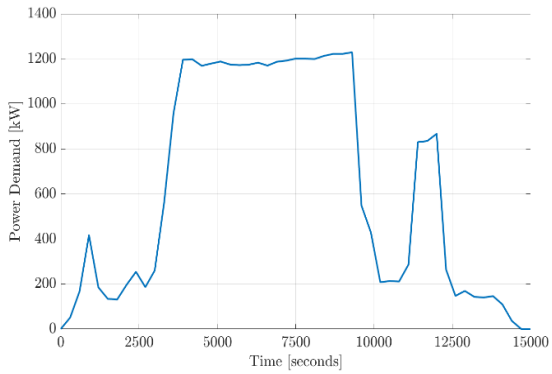

Figure 5: Power Profile for the simulations.

The battery weights for the different configurations with packs ranging from 2 to 5 units are listed in Table 4. The total weight was calculated by multiplying the module weight by the total number of modules in all packs. The total number of modules in each pack was calculated by multiplying the components connected in series with those connected in parallel.

Table 4. Number of battery packs and total weights for 550 kWh total battery capacity

Packs	Capacity of 1 pack [Ah]	Modules in each pack	Weight [tons]
2	343.7	264	7.7
3	229.2	198	8.6
4	171.8	132	7.7
5	137.5	132	9.6

Either two or four battery packs can provide 550 kWh of energy with the smallest system weight of 7.7 tons (Table 4). Hence, in each scenario, there are 2 battery packs of 275 kWh each.

Five scenarios were considered for the analysis: one for each fuel cell stack (Table 2). The total installed fuel cell power is limited to 1.2 MW which is the maximum power demanded by the diesel engine in the original mechanical version. Hence, for each scenario, the number of stacks required for onboard installation is presented in Table 5. All the fuel cells are used during operation in each scenario. No batteries or fuel cells are individually controlled and switched off during operation.

Table 5. Scenarios for different fuel cells

Scenario	Rated power (kW)	Stack no.
1	50	24
2	100	12
3	150	8
4	200	6
5	200	6

The results are presented for the power profile in Figure 5, for the 4th scenario with six fuel cell stacks of 200 kW from Powercell. The components from the different manufacturers of the fuel cells for each scenario and the nominal efficiencies at the beginning of the life cycle for each stack are presented in Table 6. Nominal efficiency is a required input parameter for the generic stack model, and for each fuel cell the nominal point is assumed to be at 80% of its rated power in this study. In two other parameterized generic stack models from the Simscape library, the nominal operating points are between 60-80% of the maximum power.

Table 6. Fuel cell nominal efficiencies

Scenario	Components	Efficiency (%)
1	Zepp.Y50	52.5
2	HyPM HD90	47.5
3	Zepp.X-150	53.5
4	Powercell-200	49.0
5	HyPM HD180	48.0

The purpose of the comparison of the different stacks is to compare the differences in fuel consumption/cost and weights for various configurations. In other words, the aim is to investigate the extent to which the hydrogen consumption and system weights vary for the same total installed power and battery capacity, but for various fuel cell component models with different parameters.

After running the simulations for the 4th scenario, the results for the DC bus voltage levels, the SoC, and the power outputs from the fuel cells and batteries were obtained.

The DC bus voltage was almost constant at 1000 V for the entire simulation time with fluctuations of less than 0.5%.

The battery SoC is shown in Figure 6. At the beginning, the SoC value remained close to the reference value of 50%. After t = 3500 seconds, the power demand increased and at approximately 4200 seconds it reached the maximum load of 1.2 MW. During the steady state, the battery SoC remained close to 40%. For the entire duration, the SoC value ranged between 35-65%, which lies within the recommended 20-80% range for degradation purposes.

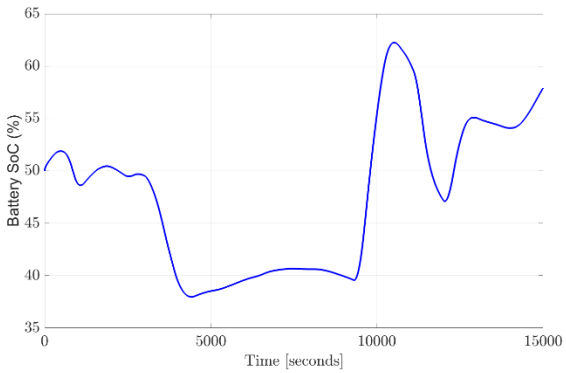

Figure 6: Battery SoC over time

In Figure 7, the power output from the fuel cells and batteries, and the analysed load profile are shown. The power losses were less than 1% for the entire voyage. The load of the fuel cells followed the power profile. A time constant of 360 seconds was used in the low-pass filter for the fuel cell current (Figure 4). Between 9,000-10,000 seconds the fuel cells provided the maximum power of 1.2 MW and the SoC is at 40% which is below the reference value of 50%. The difference between the fuel cell power and the load power in that interval is because the batteries need to be charged to reach the reference value. When the load drops, the fuel cells have extra power to charge the batteries. Between 14,500-15,000 seconds the fuel cell power converged to its lower limit which corresponds to 10% of the rated output for degradation and efficiency purposes [25]. At this interval the load profile was below the fuel cell power. If, in a different power profile, the load power was lower than the fuel cell power for a longer time interval, the battery SoC would increase until it reached the maximum limit of 80% SoC. Then, the fuel cell would have to be turned off. The condition of turning off the fuel cells is not accounted for by this strategy, but it will be considered in future work.

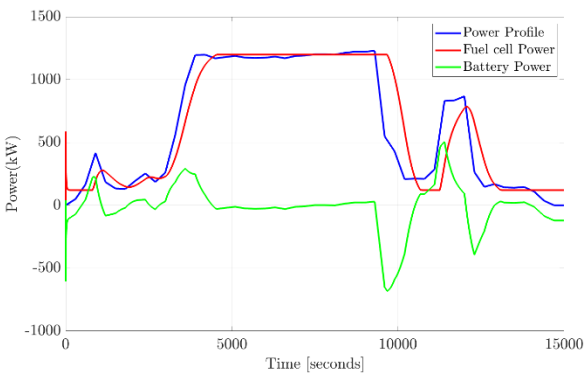

Figure 7: Power Profile vs Power output from fuel cells and batteries

A second limitation of the models and control approach is that battery efficiencies during charging and discharging were not considered. Hence, for total battery energy capacity higher or lower than the considered 550 kWh, and the same time constant in the low pass filter, the fuel consumption will remain the same, but the SoC range will change. For larger batteries, the SoC range will be smaller and for lower energy capacities than 550 kWh, the SoC range will be larger than in Figure 6.

The simulation results for the average hydrogen consumption for each of the five scenarios are summarized in Table 7. The same time constant in the low-pass filter was used for all scenarios. Hence, the differences in hydrogen consumption are due to the different fuel cell model parameters and stack efficiencies.

The detailed stack model requires the following parameters as inputs: voltage and current at 0 and 1 A, at nominal conditions and at the maximum operating point, the number of cells, nominal efficiency, nominal temperature, supply pressures of fuel and air, nominal air flow rate, and compositions of hydrogen, oxygen, and water.

The air and fuel flow rates are variable parameters that depend on the fuel cell current as shown in Equations (5) and (6) respectively, based on [17].

$$V_{air} = \frac{60{,}000RTNi_{fc}}{zFP_{air}Uf_{O2}y\%} \tag{5}$$

$$V_{fuel} = \frac{60{,}000RTNi_{fc}}{zFP_{fuel}Uf_{H2}x\%} \tag{6}$$

where V_{air} (litres/minute) and V_{fuel} (litres/minute) are the flow rates of air and fuel, R is the universal gas constant (J/molK), F is the Faraday's constant (C/mol), T is the operating temperature (K), N is the number of cells, i_{fc} is the fuel cell current which is controlled by the EMS, z is the number of moving electrons, P_{air} (atm) and P_{fuel} (atm) are the absolute supply pressures of air and fuel, Uf_{O2} and Uf_{H2} are the oxygen and hydrogen utilization rates, y% and x% are the percentages of oxygen in the oxidant and hydrogen in the fuel respectively. All the parameters on the right-hand side of (5) and (6) are assumed to be constant except for the current of the fuel cell i_{fc}.

The generic fuel cell model calculates the efficiency (η_{FC}) at various load points, as shown in (7), based on [14].

$$\eta_{FC} = \frac{P_{FC}}{V_{fuel}LHV} \tag{7}$$

where P_{FC} is the power of the fuel cell (W) at the different load points, V_{fuel} is the hydrogen flow rate calculated from (6) and converted from standard litres/minute to kg/sec, and LHV is the Lower Heating Value of hydrogen (J/kg).

Table 7. Average hydrogen consumption results

Scenario	Component	Fuel consumption [kg]
1	Zepp Y50	163.62
2	HyPM HD90	181.33
3	Zepp.X-150	162.29
4	Powercell-200	174.62
5	HyPM HD180	180.16

The lowest fuel consumption (162.29 kg) was obtained from the 3rd scenario with eight stacks Zepp.X-150 of 150 kW each, from Zepp. Solutions (Table 7). There is an 11.1 % difference with the scenario of the highest hydrogen consumption (181.33 kg), which corresponds to the case of 12 stacks of 100 kW from Hydrogenics.

At the same time interval of the considered power profile the average diesel fuel consumption of the original design was 156 kg/hour which corresponds to 649 kg of diesel required for the entire voyage of 4.16 hours. Thus, the diesel consumption was approximately 3.5-4 times higher than the hydrogen consumption, which was expected because of the Lower Heating Value of diesel, and the lower operating efficiency of the main propulsion diesel engine.

4.2 Uncertainties of fuel costs

Uncertainties have been considered for the fuel prices to investigate variations in the hydrogen cost. In Figure 8, the hydrogen price variations for 2023, based on [26], are presented using normal distribution graphs. The number of samples was set to 1,000,000, the mean was 4.5 ($/kg) and the standard deviation was 0.4472.

The vessel operates mainly in the Baltic Sea and the North Sea in European countries. It is important to note that these fuel prices are for green hydrogen production costs, so that the well-to-wake emissions are minimized. Hence, these are bare production costs and do not reflect the actual price paid by consumers, particularly when considering compressed hydrogen, liquefied hydrogen, liquid organic hydrogen carriers, or chemical hydrides. In 2023, the green hydrogen prices range between 3.5-5.5 $/kg (Figure 8) in the operational area. In general, the fuel prices in the vessel's operational area are higher than those in most parts of the world [26].

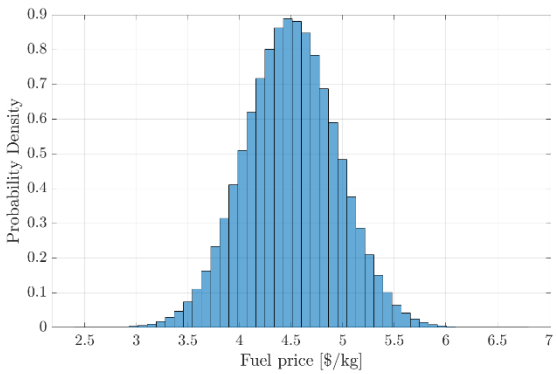

Figure 8: Hydrogen price variations for 2023

The fuel cost range ($) is presented in Figure 9. It was obtained by multiplying the fuel consumption (kg) for each scenario (Table 7) with the fuel price ($/kg) extracted from the normal distribution graph in Figure 8.

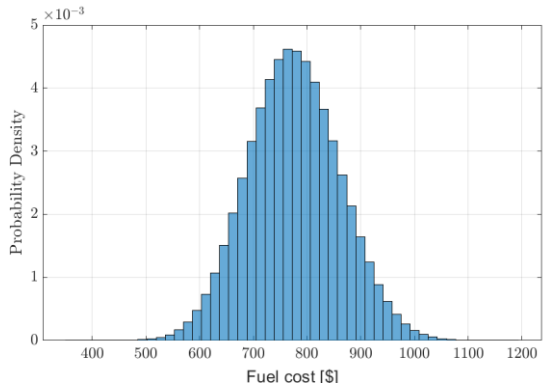

Figure 9: Fuel cost range for varying hydrogen price

Figure 10 presents the fuel cost range for each scenario with 95% confidence interval. The middle black line represents the mean (average) values, and the dotted lines represent the lower and upper limits of the fuel costs for each scenario.

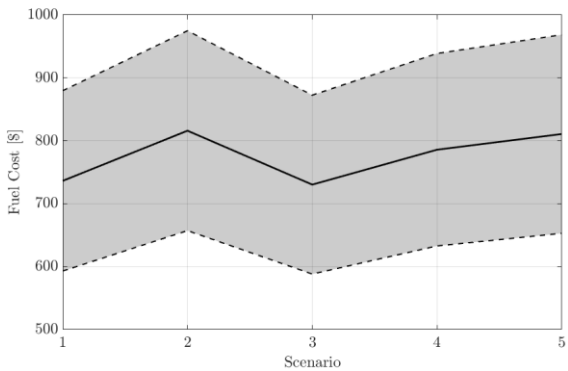

Figure 10: Fuel cost range for the 5 scenarios with 95% confidence interval

4.3 Average fuel costs vs weights

The solutions for the five scenarios, in terms of weight and average fuel cost, are presented in Table 8 and Figure 11.

Table 8. Fuel cost and weight for each scenario

Scenario	Fuel cost [$]	Weight [tons]
1	736.3	12.78
2	816.0	11.62
3	730.3	10.54
4	785.8	14.12
5	810.7	11.62

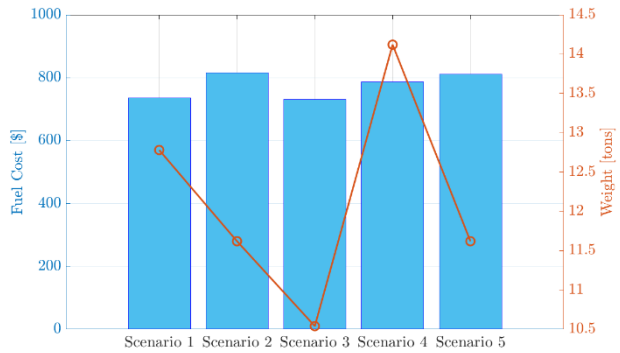

Figure 11: Weight-average fuel cost solutions for each scenario for 2023 hydrogen prices

It can be observed in Figure 11 that the configuration with eight stacks of 150 kW (Scenario 3) has the lowest total fuel cost (730 $) with an average difference of 7.1% from the other solutions, and the lowest total weight (10.54 tons) with an average difference of 15.4% from the other solutions.

The weight of the original diesel engine is equal to 11.6 tons. The weight of the considered fuel cells and batteries in the retrofitted version ranges between 10.54 – 14.12 tons from the five scenarios (Figure 11). The system weight of the hydrogen-hybrid version for the 3rd scenario is 1 ton less than that of the original system, without considering other components, apart from the main equipment that provides the propulsion loads.

5. CONCLUSIONS

This research focused on alternative energy sources in marine systems, specifically on a hydrogen-fuelled vessel, with hybrid power supply, obtained by conceptual retrofitting of a diesel-based cargo vessel.

Our work included a modelling and control study for the hypothetical retrofitting employing fuel cell, battery, and converter models that can be adapted for various power plant sizes and ship types, making our approach highly versatile.

The fuel cells and batteries were sized based on the most power and energy intensive (fluctuating) power profiles, but the modelling and control results were presented for a short voyage of approximately 4 hours for computational requirements. The developed robustly coordinated control strategy, which can be applied to different vessel power profiles, resulted in less than 0.5% DC bus voltage fluctuations from its reference value, and a battery SoC range of 35-65% by efficiently splitting the power between the fuel cells and batteries with power losses of less than 1% for the entire voyage.

A database of five fuel cell stacks, from different manufacturers, was considered in this model-based parametric study to investigate different combinations in terms of fuel consumption, cost, and weight. The fuel cost range was estimated with a 95% confidence interval for each case by multiplying the fuel price from the normal distribution graph (3.5-5.5 $/kg for 2023) with the hydrogen consumption for each scenario. Overall, the 3rd scenario with eight stacks/150 kW from Zepp. Solutions resulted in the lowest fuel cost of 703$ with an average difference of 7.1% from the other solutions. This configuration also resulted in the lowest combined fuel cell and battery system weight of 10.54 tons, which is 1 ton lighter than that of the original diesel engine.

In future work, an optimization algorithm will be implemented for the sizing and control problem, considering capital costs, system volumes, and component degradation. An optimization algorithm will explore a larger design space. Inverters, motors, and propeller models will also be developed, and a lifecycle analysis of the emissions and costs will be conducted.

ACKNOWLEDGEMENT

This research was supported by the Sustainable Hydrogen Integrated Propulsion Drives (SH2IPDRIVE) project, which has received funding from RvO (reference number MOB21013) through the RDM regulation of the Ministry of Economic Affairs and Climate Policy.

Rijksdienst voor Ondernemend Nederland

SH2IPDRIVE
HYDROGEN FOR MARITIME

REFERENCES

[1] D. Gritsenko, "Regulating GHG Emissions from shipping: Local, global, or polycentric approach?", *Mar. Policy*, vol. 84, pp. 130–133, Oct. 2017.

[2] S. Fang, Y. Wang, B. Gou and Y. Xu, "Toward future green maritime transportation: An overview of seaport microgrids and all-electric ships", *IEEE Trans. Veh. Technol.*, vol. 69, no. 1, pp. 207-219, Jan. 2020.

[3] O. B. Inal, J. F. Charpentier and C. Deniz, "Hybrid power and propulsion systems for ships: Current status and future challenges", *Renewable and Sustain. Energy Rev.*, vol. 156, Mar. 2022.

[4] J. Zhu, L. Chen, B. Wang and L. Xia, "Optimal design of a hybrid electric propulsive system for an anchor handling tug supply vessel", *Appl. Energy*, vol. 226, pp. 423-436, Sept. 2018.

[5] J. Zhu, L. Chen, B. Wang and L. Xia, "Bi-objective optimal design of plug-in hybrid electric propulsion system for ships", *Energy*, vol. 177, pp. 247-261, Jun. 2019.

[6] T. L. Vu, A. A. Ayu, J. S. Dhupia, L. Kennedy and A. K. Adnanes, "Power Management for Electric Tugboats Through Operating Load Estimation", *IEEE Trans. on Control Syst. Technol.*, vol. 23, no. 6, pp. 2375–2382, Nov. 2015.

[7] F. D. Kanellos, "Optimal power management with GHG emissions limitation in all-electric ship power systems comprising energy storage systems". *IEEE Trans. Power Syst.*, vol. 29, no. 1, pp. 330-339, Jan. 2014.

[8] F. D. Kanellos, A. Anvari-Moghaddam and J. M. Guerrero, "A cost-effective and emission-aware power management system for ships with integrated full electric propulsion", *Electric Power Syst. Res.*, vol. 150, pp. 63-75, Sept. 2017.

[9] Z. Wang and X. Li, "Research on multi-objective optimization of capacity allocation for marine hybrid energy storage systems", in *Proc. IOP Conf. Ser: Earth Environ. Sci.*, vol. 692, 1st ed., Mar. 2021.

[10] C. Chen, X. Wang and J. Xiao, "An energy allocation strategy for hybrid ship DC power system based on genetic algorithm", *IETE J. Res.*, vol. 62, no. 3, pp. 301-306, Oct. 2015.

[11] L. Balestra and I. Schjølberg, "Modelling and simulation of a zero-emission hybrid power plant for a domestic ferry", *Int. J. Hydrogen Energy*, vol. 46, no. 18, pp. 10924-10938, Mar. 2021.

[12] L. Balestra and I. Schjølberg, "Energy management strategies for a zero-emission hybrid domestic ferry", *Int. J. Hydrogen Energy*, vol. 46, no. 77, pp. 38490-38503, Nov. 2021.

[13] T. Jaster, A. Rowe and Z. Dong, "Modeling and simulation of a hybrid electric propulsion system of a green ship", in *Proc. 10th IEEE/ASME Int. Conf. Mechatronic Embedded Syst Appl. (MESA)*, Senigallia, Italy, Sept. 10-12, 2014, pp. 1-6.

[14] M. Cha *et al.*, "Power Management Optimisation of a Battery/Fuel Cell Hybrid Electric Ferry", in *Proc. 31st Australasian Univ. Power Eng. Conf. (AUPEC)*, Perth, Australia, Sept. 26-30, 2021.

[15] A. M. Bassam, A. B. Philips, S. R. Turnock and P. A. Wilson, "Development of a multi-scheme energy management strategy for a hybrid fuel cell driven passenger ship", *Int. J. Hydrogen Energy*, vol. 42, no. 1, pp. 623-635, Jan. 2017.

[16] A. M. Bassam, A. B. Philips, S. R. Turnock and P. A. Wilson, "An improved energy management strategy for a hybrid fuel cell/battery passenger vessel", *Int. J. Hydrogen Energy*, vol. 41, no. 47, pp. 22453–22464, Dec. 2016.

[17] N. M. Souleman, O. Tremblay and L. A. Dessaint, "A generic fuel cell model for the simulation of fuel cell vehicles", in *Proc. 5th IEEE Veh. Power and Propulsion Conf. (VPPC)*, Dearborn, MI, USA, Sept. 7-10, 2009.

[18] O. Tremblay, L. A. Dessaint and A. I. Dekkiche, "A Generic Battery Model for the Dynamic Simulation of Hybrid Electric Vehicles", in *Proc. 4th IEEE Veh. Power and Propulsion Conf. (VPPC)*, Arlington, TX, USA, Sept. 9-12, 2007.

[19] K. Kwon, D. Park and M. K. Zadeh, "Load Frequency-Based Power Management for Shipboard DC Hybrid Power Systems", in *Proc. 29th IEEE Int. Symp. Ind Electron. (ISIE)*, Delft, Netherlands, Jun. 17-19, 2020, pp. 142–147.

[20] W. Yeetum and V. Kinnares, "PI Controller Based on Direct Synthesis Method for DC-Link Voltage Control of Active Power Filter", in *Proc. Int. Elect. Eng. Congr. (IEECON)*, Krabi, Thailand, Mar. 7-9, 2018.

[21] Maritime hydrogen fuel cell systems - zepp.solutions, https://zepp.solutions/en/maritime-fuel-cell-systems/ (accessed Feb. 1, 2023).

[22] Accelera | Powering the World with Clean Energy, https://www.accelerazero.com/ (accessed Feb. 5, 2023).

[23] Marine | PowerCell Group | Hydrogen Fuel Cell Solutions, https://powercellgroup.com/segments/marine (accessed Feb. 10, 2023).

[24] M. Boekhout, "Hydrogen Powered Ship Propulsion for High-Speed Craft: The implementation of Fuel Cell Battery Propulsion Systems", M.S. Thesis, Dept. 3mE, Delft Univ. of Technol., Delft, Netherlands, 2020.

[25] X. Wang *et al.*, "Sizing and Control of a Hybrid Ship Propulsion System Using Multi-Objective Double-Layer Optimization", *IEEE Access*, vol. 9, pp. 72587–72601, May 2021.

[26] Green hydrogen economy - predicted development oftomorrow:PwC, https://www.pwc.com/gx/en/industries/energy-utilities-resources/future-energy/green-hydrogen-cost.html (accessed Feb. 10, 2023).